

Aquifer parameter identification using the extended Kalman filter

C. H. Leng and H. D. Yeh

Institute of Environmental Engineering, National Chiao-Tung University, Hsinchu, Taiwan

Received 6 August 2001; revised 30 October 2002; accepted 30 October 2002; published 19 Month 2003.

[1] An approach using the extended Kalman filter (EKF) and cubic spline is proposed to identify the aquifer parameters in both confined and unconfined aquifer systems. The cubic spline applied to the observation data can generate interpolated data with uniform time intervals and facilitates the implementation of EKF. The EKF combined with the Theis solution or Neuman's model, using the interpolated drawdown data produced by cubic spline, can optimally determine the parameters through the recursive process. The proposed approach can quickly identify the parameters, using only part of observed drawdown data, and the obtained parameters are shown to have good accuracy. Thus length of time of pumping tests may be shortened. Comparisons of results from nonlinear least squares combined with finite difference Newton's method (NLN) and EKF show that the EKF allows a wider range of initial guess values than NLN and have the accuracy of the results on the same order of magnitude as that of NLN. When determining the aquifer parameters, the identification process of specific yield reflects the effect of gravity drainage on the drawdown curve and conforms to the physical nature of an unconfined aquifer. Furthermore, this study shows that EKF can be successfully applied to analyze the drawdown data even with white noises or temporally correlated noises. *INDEX TERMS:* 1829 Hydrology: Groundwater hydrology; 1869 Hydrology: Stochastic processes; 1899 Hydrology: General or miscellaneous; *KEYWORDS:* parameter estimation, Kalman filter, cubic spline, groundwater, confined aquifer, unconfined aquifer

Citation: Leng, C. H., and H. D. Yeh, Aquifer parameter identification using the extended Kalman filter, *Water Resour. Res.*, 39(3), 1062, doi:10.1029/2001WR000840, 2003.

1. Introduction

[2] In the past, analysis of pumping test data in a confined aquifer was usually made using a graphical procedure with the type curve plotted from a Theis nonequilibrium formula. *Theis* [1935] obtained the solution for unsteady groundwater flow toward a well in a confined aquifer by analogy to the problem of heat conduction. *Cooper and Jacob* [1946] developed an approximation for the Theis equation, together with a data analysis method which does not require type-curve matching. *Chow* [1952] presented a graphical method based on the Theis equation to obtain the transmissivity and storage coefficient of a confined aquifer. *Boulton* [1954, 1963] developed the analytical solution by introducing the concept of delayed yield for unconfined formations. *Prickett* [1965] described a systematic approach to determine the parameters, using a graphical procedure based on Boulton's type of curves. *Cooley and Case* [1973] showed that Boulton's equation yields an exact solution where it describes a flow system with a rigid phreatic aquitard on top of the main aquifer, and the unsaturated flow above the phreatic surface is neglected. *Neuman* [1972, 1974] presented a solution that considers the effects of elastic storage and anisotropy of aquifers on drawdown behavior. Neuman's model treated the unconfined aquifer as a compressible system and the phreatic surface as a moving boundary. His theory was also extended to account for the

effect of a partially penetrating pumping well or/and an observation well in a homogeneous anisotropic unconfined aquifer. *Neuman* [1975] also gave a graphical type curve solution procedure to determine the hydraulic parameters. *Moench* [1995] combined the Boulton and Neuman models for flow toward a well in an unconfined aquifer.

[3] *Yeh* [1987] used the nonlinear least squares and finite difference Newton's method (NLN) for identifying the parameters of the confined aquifer. *Huang* [1996] used NLN to identify the unconfined hydraulic parameters. This approach also was applied to the cases of partial penetration of pumped or/and observed wells, whereas the graphical method was only suitable for analyzing the hydraulic parameters under the condition of a fully penetrating well. Their approach has the advantage of high accuracy and quick convergence for most initial guesses when estimating the hydraulic parameters via pumping test data. For other numerous computation methods, refer to *Yeh* [1987] for a literature review.

[4] Works using the Kalman filter for the hydraulic parameters and water table related estimations may be divided into two categories. One applies the Kalman filter in a linear system [e.g., *Van Geer and Van Der Kloet*, 1985; *Van Geer and te Stroet*, 1990; *Van Geer et al.*, 1990; *Lee et al.*, 2000; *Bierkens et al.*, 2001] and the other deals with nonlinear problems using the extended Kalman filter (EKF) [e.g., *Chander et al.*, 1981; *Katul et al.*, 1993; *Bierkens*, 1998; *Cahill et al.*, 1999]. *Chander et al.* [1981] employed the iterated extended Kalman filter to estimate the parameters for both nonleaky and leaky aquifers. Regarding the

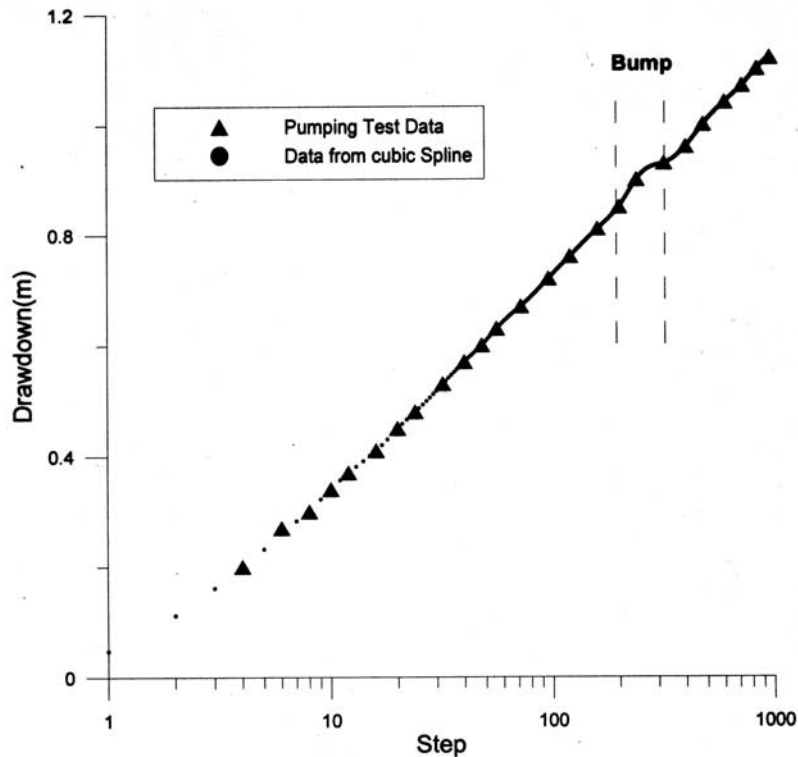


Figure 1. Pumping test data and interpolation data by cubic spline for the confined aquifer.

nonleaky aquifer, the measurement equation uses a truncated form of Theis' well function, which might be incorrect in predicting drawdown when the pumping time is short. Van Geer and Van Der Kloet [1985] presented two linear, filter-based schemes for parameter estimation in groundwater flow problems. An optimal estimate was simultaneously computed for the original state, i.e., heads and the parameter state. Van Geer and te Stroet [1990] incorporated MODFLOW into a filtering framework and updated the prior estimates of hydraulic parameter values using an off-line procedure, when minimizing the difference between the actual head measurements and those predicted from the MODFLOW-Kalman filter framework. Van Geer et al. [1990] also raised the idea of using a filter for state estimation in the absence of significant dynamic behavior and they investigated the applicability of the filter to a relatively swiftly reacting groundwater system. Katul et al. [1993] used the EKF to test for the determination of the hydraulic conductivity function from a field drainage experiment. Bierkens [1998] embedded the stochastic differential equation (SDE) in the EKF algorithm to calibrate the parameters and noise statistics of SDE on a time series of water table depths. Eigbe et al. [1998] reviewed the difficulties associated with using a filter with groundwater flow models, and identified procedures that would facilitate its more effective and convenient use in this field. Cahill et al. [1999] proposed a method for deriving optimal parameters for an effective large-scale hydraulic conductivity that considers both the temporal and spatial variations of the moisture content. Lee et al. [2000] applied a linear Kalman filter to identify the anisotropic aquifer transmissivity and storage coefficient of a confined aquifer, using Cooper and Jacob's equation and Popadopoulos' approach. Unfortu-

nately, their approach is applicable only when the argument of the well function is less than 0.01, and the observed data must be measured in uniform time intervals, which is impractical in field applications. Bierkens et al. [2001] modeled the spatiotemporal variation of shallow water table depth with a regionalized version of an autoregressive exogenous (ARX) time series model. The regionalized ARX parameters were estimated by embedding the regionalized ARX model in a space-time Kalman filter.

[5] The current study presents a new approach that uses the EKF to determine the parameters of confined and unconfined aquifer systems. Reasonable guess values for both confined and unconfined aquifer parameters may be made based on the field aquifer hydrogeology and the experiences of a hydrologist. With the initial guesses of the parameters and the data interpolated from the observed drawdowns, the EKF algorithm will proceed step by step to optimally identify the system parameters. In a confined aquifer, the EKF coupled with the Theis solution is used to first estimate the drawdown and then determine the values of transmissivity and storage coefficient at each filtering step k . On the other hand, the EKF combined with Neuman's model for an unconfined aquifer works in the same manner as that of confined aquifer and determines the values of vertical and radial hydraulic conductivities, specific storage, and specific yield at each step. The field-observed drawdown data usually have nonuniform time intervals. Therefore the cubic spline method is applied to generate the interpolated data with uniform time interval. This interpolation approach can facilitate the application of the EKF.

[6] In contrast to previous researches, in this study the state vector is comprised of the hydraulic parameters and the model, i.e., the Theis solution or Neuman's model, is

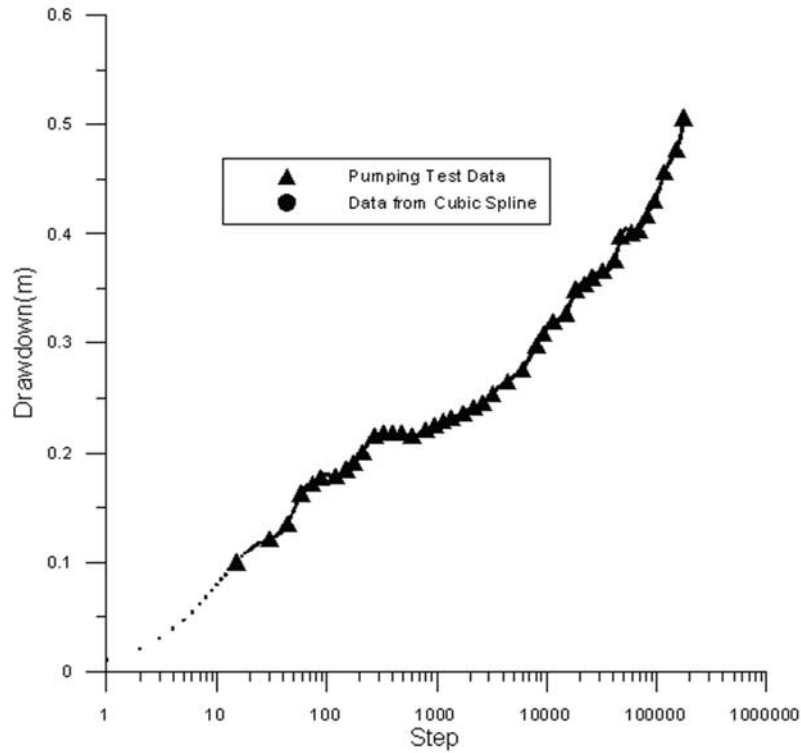


Figure 2. Pumping test data and interpolation data by cubic spline for the unconfined aquifer.

used as the measurement equation. The unknown parameters are thus estimated on-line as the observations come in. This approach could be implemented on a computer, which could be linked to a data logger and a pressure transducer that measures the water level in the observation well during a pumping test. The desired hydraulic parameters can then be estimated in the field on-line and once stable estimates have been obtained, the pumping test may be terminated.

2. Methodology

[7] This section includes two parts: the theoretical framework of extended Kalman filter and cubic spline.

2.1. Discrete Extended Kalman Filter

[8] A system for the state vector described by the dynamic model is presented by *Grewal and Andrews* [1993] as

$$x_k = f(x_{k-1}, k-1) + w_k \quad (1)$$

where x_{k-1} and x_k are respectively the state vector at time steps $k-1$ and k , $f(x_{k-1}, k-1)$ is the nonlinear function for the state vector, and w_k is the state noise assumed to be normally distributed with zero mean white (uncorrelated) sequence with known covariance structure Q_k . Notably, the state vector denotes the hydraulic parameters, and Q_k is assumed to be a zero vector throughout the filtering steps.

[9] The estimate for the state vector is of similar form as (1)

$$\hat{x}_k(-) = f(\hat{x}_{k-1}(+), k-1) \quad (2)$$

where $\hat{x}_k(-)$ denotes the prior (or a priori) estimate at k step and $\hat{x}_{k-1}(+)$ represents the posterior (or a posteriori)

estimate at $k-1$ step. This dynamic system may predict the state estimate which can be used to obtain the predicted measurement \hat{z}_k .

[10] A system measurement model may be represented as [*Grewal and Andrews*, 1993]

$$z_k = h(x_k, k) + v_k \quad (3)$$

where z_k is the measurement vector at time step k , and $h(x_k, k)$ is the nonlinear function for the measurement system. Uncorrelated with w_k sequence, v_k is the measurement noise assumed to be a white sequence with the known covariance matrix R_k . The matrix R_k is assumed to be constant throughout the filtering process. Herein the nonlinear function is represented by the drawdown equation (e.g., the Theis solution or Neuman's model), which is considered as a function of the hydraulic parameters.

[11] To obtain the predicted measurement, an expression similar to (3) is

$$\hat{z}_k = h(\hat{x}_k(-), k) \quad (4)$$

[12] For this, an initial estimate of the process at some point in time step k is required. The estimate can be made based on all available knowledge about the process prior to time step k . The error covariance matrix associated with $\hat{x}_k(-)$ is also assumed to be known. The prior estimation error $e_k(-)$ is defined as $x_k - \hat{x}_k(-)$. The a priori error covariance matrix of $x_k - \hat{x}_k(-)$, denoted as $P_k(-)$, is

$$P_k(-) = E[e_k(-)e_k^T(-)] = E[(x_k - \hat{x}_k(-))(x_k - \hat{x}_k(-))^T] \quad (5)$$

Table 1. Results of Parameter Estimation by EKF With Various Initial Guesses for T and S

Case	Initial Guess		NS ^a	Convergence	Estimated Values		Errors	
	T , m ² /day	S			T , m ² /day	$S \times 10^{-4}$	ME $\times 10^{-3}$	SEE $\times 10^{-3}$
1	700	0.001	568	yes	1158	1.76	-6.47	9.69
2	700	0.0001	500	yes	1144	1.88	-1.76	5.90
3	700	0.00001	-	no	-	-	-	-
4	1300	0.001	477	yes	1164	1.74	-5.67	9.85
5	1300	0.0001	512	yes	1140	1.90	-1.79	5.78
6	1300	0.00001	-	no	-	-	-	-
7	2000	0.001	-	no	-	-	-	-
8	2000	0.0001	535	yes	1136	1.91	-0.96	5.57
9	2000	0.00001	-	no	-	-	-	-

^aNS represents the number of time steps, with each time step equal to 15 s.

The a posteriori covariance $P_k(+)$, indicating the error covariance matrix after update, can be defined in a similar manner.

[13] With the assumption of the a priori estimate $\hat{x}_k(-)$, the measurement z_k is used to improve the prior estimate

$$\hat{x}_k(+) = \hat{x}_k(-) + \bar{K}_k(z_k - \hat{z}_k) \quad (6)$$

where \bar{K}_k is defined as the Kalman gain and $\hat{x}_k(+)$ is the update estimate at step k . The updated state vector $\hat{x}_k(+)$ can be substituted back to (2) to form a new estimate $\hat{x}_{k+1}(-)$ at step $k + 1$. The Kalman filter uses minimum mean square error as the performance criterion to find the particular \bar{K}_k that yields an updated estimate. The Kalman gain is sought to make $\hat{x}_k(+)$ satisfy the orthogonality principle, thus minimizing the square errors. Detailed derivations of the minimization process are presented by *Grewal and Andrews* [1993].

[14] The particular \bar{K}_k that minimizes the mean square estimation error is

$$\bar{K}_k = P_k(-)H_k^T [H_k P_k(-)H_k^T + R_k]^{-1} \quad (7)$$

where the measurement matrix H_k is approximated by the derivative of the right-hand side of (4) and may be expressed as

$$H_k \approx \left. \frac{\partial h(x, k)}{\partial x} \right|_{x=\hat{x}_k(-)} \quad (8)$$

[15] The error covariance matrix associated with the updated (a posteriori) estimate is

$$P_k(+) = [I - \bar{K}_k H_k] P_k(-) \quad (9)$$

where $P_k(+)$ denotes the error covariance updated by the Kalman gain and I represents an identity matrix. Both the prior and update error covariance matrices would remain symmetric and positive definite [*Grewal and Andrews*, 1993].

[16] Derived from (5), the error covariance matrix may also be expressed as

$$P_k(-) = \Phi_{k-1} P_{k-1}(+) \Phi_{k-1}^T + Q_{k-1} \quad (10)$$

where the state transition matrix, Φ_{k-1} , expressed as the derivative of the state vector estimation equation is

$$\Phi_{k-1} \approx \left. \frac{\partial f(x, k-1)}{\partial x} \right|_{x=\hat{x}_{k-1}(-)} \quad (11)$$

[17] The computational procedure for the EKF is executed in a recursive manner. First, $P_k(-)$ in (10) is calculated by using the updated $P_{k-1}(+)$ at previous steps, Φ_{k-1} and Q_{k-1} . Second, Kalman gain \bar{K}_k in (7) is computed by introducing the previously calculated $P_k(-)$, H_k , and R_k . Then, $P_k(+)$ in (9) is evaluated by inserting \bar{K}_k from the second step and $P_k(-)$ from the first step. Finally, the successive values of $\hat{x}_k(+)$ in (6) are computed by using the known \bar{K}_k , $\hat{x}_k(-)$, and the input data z_k . The convergence criterion to terminate the recursive process may be written as

$$|x_{k+1} - x_k| < \text{TOL}_x \quad (12)$$

where TOL_x represents the specified tolerance. Once the process is terminated, the convergent values of the parameters are obtained.

2.2. Cubic Spline

[18] A set of third-degree polynomials, y_i between each pair of adjacent data points from x_i to x_{i+1} , is considered. An interpolating polynomial that passes through all the points is continuous in its slope. Due to the condition that the slopes of the two cubics that join at (x_i, y_i) are the

Table 2. Results of Parameters Estimation by EKF With $S = 10^{-4}$ and T Ranging From 100 to 3000 m²/day

Initial Guess T , m ² /day	NS ^a	Estimated Values		Errors	
		T , m ² /day	$S \times 10^{-4}$	ME $\times 10^{-3}$	SEE $\times 10^{-3}$
100	481	1157	1.79	-4.11	8.09
500	171	1140	1.92	-0.03	5.47
1000	504	1143	1.89	1.32	5.72
1500	517	1139	1.91	-1.36	5.64
2500	194	1134	1.95	-0.12	5.54
3000	807	1139	1.92	-0.47	5.48

^aNS represents the number of time steps, with each time step equal to 15 s.

same, a general expression for cubic spline is obtained as [Gerald and Wheatley, 1994; Burden and Faires, 1997]

$$h_{i-1}S_{i-1} + 2(h_{i-1} + h_i)S_i + h_iS_{i+1} = 6 \left(\frac{y_{i+1} - y_i}{h_i} - \frac{y_i - y_{i-1}}{h_{i-1}} \right) \quad (13)$$

where $h_i = x_{i+1} - x_i$ is the width of i th interval and S_i represents the second derivative at the point (x_i, y_i) . Equation (13) can produce a new data set with uniform time intervals by interpolating the original data with nonuniform time intervals. Note that the x coordinate and the y coordinate represent the time since pumping started and the drawdown, respectively.

3. Application of EKF and Cubic Spline

[19] This section illustrates how a Kalman filter is coupled with the Theis solution or Neuman's model to identify hydraulic parameter. The parameters of transmissivity, T , and storage coefficient, S , of the confined aquifer are optimally determined when employing the EKF at each filtering step k to analyze the interpolated drawdown data. The parameters of radial hydraulic conductivity K_r , vertical hydraulic conductivity K_z , storage coefficient S , and specific yield S_y of the unconfined aquifer can also be estimated in a similar manner.

3.1. Application of Discrete EKF to a Confined Aquifer

3.1.1. Dynamic and Measurement Models for the Theis Solution

[20] Both T and S denote the state vector to be determined at each time step. The state vector from (2) may be expressed as

$$\hat{x}_k(-) = \begin{bmatrix} \hat{T}_k(-) \\ \hat{S}_k(-) \end{bmatrix} \quad (14)$$

[21] After each time step, the renewed state vector in (14) is substituted into the Theis solution, consequently forming the estimated drawdown. Based on Theis [1935] the estimated drawdown \hat{x}_k from (4) may be written as

$$\hat{z}_k = \frac{q}{4\pi T} W(u) \quad (15)$$

and

$$u = \frac{r^2 S}{4Tt} \quad (16)$$

where q is the pumping rate, $W(u)$ is the well function, r is the distance between pumping well and observation well, and t is the time since pumping started. The well function may be expressed as

$$W(u) = \left[-0.5772157 - \ln u - \sum_{n=1}^{\infty} (-1)^k \frac{u^n}{n \cdot n!} \right] \quad (17)$$

The high order terms of u in (17) may be truncated when $u^n / (n \cdot n!)$ is less than 10^{-7} .

3.1.2. Linear Approximation Equations for the Theis Solution

[22] The first-order approximation for the transition matrix from (11) is given as

$$\Phi_{k-1} \approx \begin{bmatrix} \frac{\partial T}{\partial T} & \frac{\partial T}{\partial S} \\ \frac{\partial S}{\partial T} & \frac{\partial S}{\partial S} \end{bmatrix} \quad (18)$$

[23] Based on (10), $P_k(-)$ can be estimated with known transition matrix Φ_{k-1} . Obviously, Φ_{k-1} in (18) is an identity matrix, thus simplifying the calculation of $P_k(-)$. With the assumption that Q_{k-1} equals zero, (10) may reduce to

$$P_k(-) = P_{k-1}(+) \quad (19)$$

[24] To update the hydraulic parameters in (6), the Kalman gain \bar{K}_k , estimated by known H_k and the prior covariance matrix $P_k(-)$, is first required. The input z_k that appeared in (6) denotes the interpolated drawdown data generated by cubic spline. The measurement matrix H_k from (8) consists of two elements. These are the partial derivatives of the estimated drawdown \hat{x}_k with respect to T and S , respectively, that is

$$H_k \approx \begin{bmatrix} \frac{\partial \hat{z}_k}{\partial T} & \frac{\partial \hat{z}_k}{\partial S} \end{bmatrix} \quad (20)$$

The evaluation of (20) is described in Appendix A.

3.2. Application of Discrete EKF to an Unconfined Aquifer

3.2.1. Dynamic and Measurement Models for Neuman's Solution

[25] The state vector containing the parameters of the unconfined aquifer in (2) at each time step is

$$\hat{x}_k(-) = [\hat{K}_{rk}(-) \hat{K}_{zk}(-) \hat{S}_k(-) \hat{S}_{yk}(-)]^T \quad (21)$$

[26] After each time step, the renewed state vector $\hat{x}_k(-)$ from (21) is substituted into Neuman's model, consequently forming the estimated drawdown \hat{x}_k . The estimated measurement \hat{x}_k of (4) is expressed as [Neuman, 1974]

$$\hat{z}_k = \frac{q}{4\pi T} \int_0^{\infty} 4yJ_0(y\beta^{1/2}) \left[u_0(y) + \sum_{n=1}^{\infty} u_n(y) \right] dy \quad (22)$$

where $T = K_r b$, b is the initial saturated thickness, $J_0(x)$ is a zero order Bessel function of the first kind, $\beta = K_z r^2 / K_r b^2$ is a dimensionless parameter, y is a dummy variable, and

$$u_0(y) = \frac{\{1 - \exp[-t_s \beta (y^2 - r_0^2)]\} \cosh(r_0 z_D)}{[y^2 + (1 + \sigma)r_0^2 - (y^2 - r_0^2)^2 / \sigma] \cosh(r_0)} \cdot \frac{\sinh[r_0(1 - d_D)] - \sinh[r_0(1 - l_D)]}{(l_D - d_D) \sinh(r_0)} \quad (23)$$

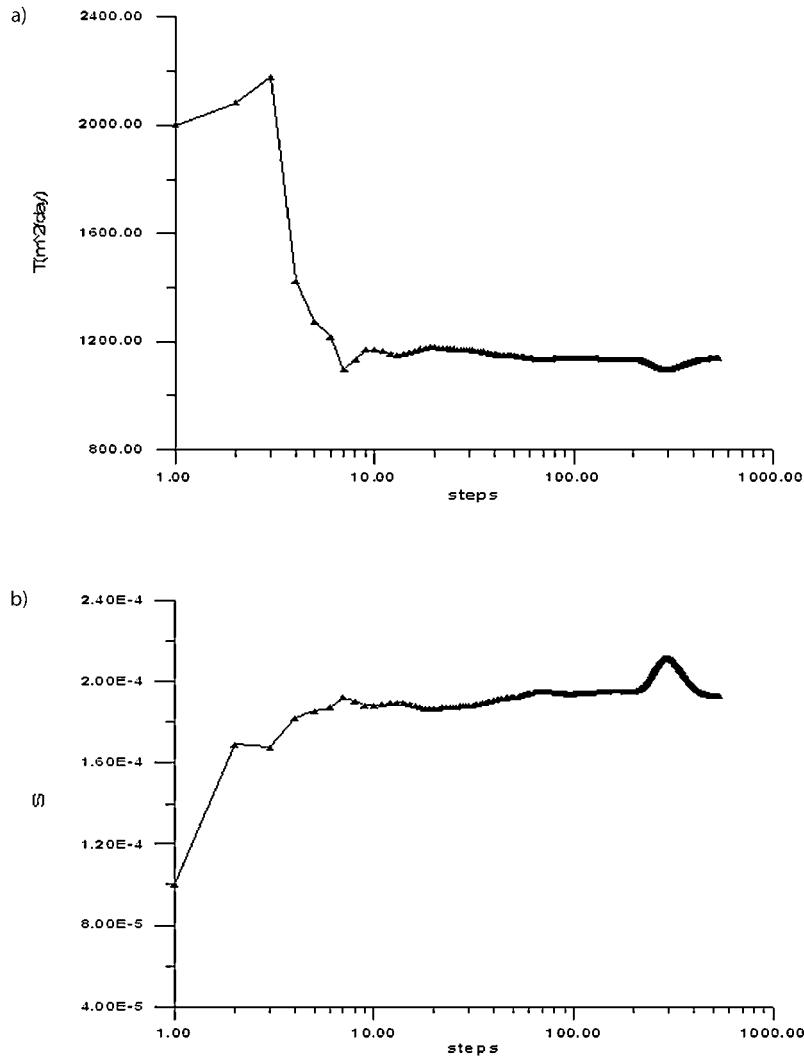


Figure 3. Parameter identification process of the confined aquifer for (a) T and (b) S .

$$u_n(y) = \frac{\{1 - \exp[-t_s \beta (y^2 + r_n^2)]\} \cos(r_n z_D)}{[y^2 - (1 + \sigma)r_n^2 - (y^2 + r_n^2)^2 / \sigma] \cos(r_n)} \cdot \frac{\sin[r_n(1 - d_D)] - \sin[r_n(1 - l_D)]}{(l_D - d_D) \sin(r_n)} \quad (24)$$

where $t_s = Tt/Sr^2$ represents the dimensionless time since pumping started, z_D is the dimensionless elevation of observation point, $\sigma = S/S_y$ is a dimensionless parameter, d_D denotes the dimensionless vertical distance between the top of perforation in the pumping well and the initial position of water table, and l_D is the dimensionless vertical distance between the bottom of perforation in the pumping well and the initial position of water table. The terms of r_0 and r_n are respectively the roots of the following two equations

$$\sigma r_0 \sinh(r_0) - (y^2 - r_0^2) \cosh(r_0) = 0, \quad r_0^2 < y^2 \quad (25)$$

and

$$\sigma r_n \sin(r_n) + (y^2 + r_n^2) \cos(r_n) = 0, \quad (2n - 1)(\pi/2) < r_n < n\pi \quad (26)$$

3.2.2. Linear Approximation Equations for Neuman's Model

[27] The first-order approximation for the transition matrix in (11) is given as

$$\Phi_{k-1} \approx \begin{bmatrix} \frac{\partial K_r}{\partial K_r} & \frac{\partial K_r}{\partial K_z} & \frac{\partial K_r}{\partial S} & \frac{\partial K_r}{\partial S_y} \\ \frac{\partial K_z}{\partial K_r} & \frac{\partial K_z}{\partial K_z} & \frac{\partial K_z}{\partial S} & \frac{\partial K_z}{\partial S_y} \\ \frac{\partial S}{\partial K_r} & \frac{\partial S}{\partial K_z} & \frac{\partial S}{\partial S} & \frac{\partial S}{\partial S_y} \\ \frac{\partial S_y}{\partial K_r} & \frac{\partial S_y}{\partial K_z} & \frac{\partial S_y}{\partial S} & \frac{\partial S_y}{\partial S_y} \end{bmatrix} \quad (27)$$

which is in fact an identity matrix facilitating the calculation of $P_k(-)$. The relation between $P_k(-)$ and $P_{k-1}(+)$ is also described by (19). The measurement matrix H_k and the prior covariance matrix $P_k(-)$ are used to determine the Kalman gain. Both H_k and $P_k(-)$ should be calculated in advance by (8) and (10), respectively. The input z_k is the measurement data produced by cubic spline. The measurement matrix H_k is composed of $\partial \hat{x}_k / \partial K_r$, $\partial \hat{x}_k / \partial K_z$, $\partial \hat{x}_k / \partial S$, and $\partial \hat{x}_k / \partial S_y$,

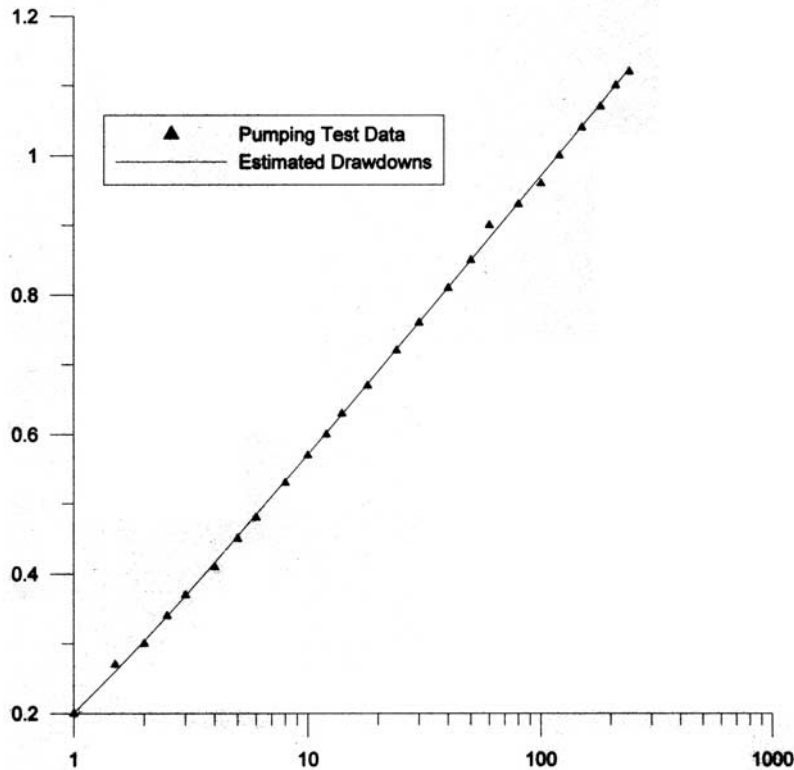


Figure 4. Comparison of the pumping test data from *Todd* [1980, p. 127] and the drawdowns estimated by using the identified confined aquifer parameters.

which can be approximated by forward difference. Detailed descriptions on the approximation are also provided in Appendix A.

3.3. Application of Cubic Spline to Drawdown Data

[28] The drawdown data obtained from field aquifer tests are normally nonuniform in time intervals, which leads to difficulties for implementation of Kalman filters. Therefore a cubic spline is applied to the observation data to generate interpolated data with uniform time intervals.

[29] A pumping test performed in a confined aquifer with a fully penetrating well was taken from *Todd* [1980, p. 127]. This well was pumped at a uniform rate of 2500 m³/day and the drawdown was measured in an observation well 60 m away from the pumping well. The uniform time interval for drawdowns in the confined aquifer obtained by using a cubic spline is 15 s for each step. The pumping test with 26 data points lasted 240 min (4 hours), which means that there are 960 interpolated drawdown data points generated by the cubic spline. Therefore a total of 960 time steps are available for EKF identification process. Figure 1 illustrates both the interpolated data produced by cubic spline and the original observed drawdown data, showing a bump between time steps 200 and 320, i.e., 50 and 80 min since pumping started. The rest of the data points seem to follow Their behavior.

[30] The pumping test for an unconfined aquifer was done in 1965 by the Bureau of Geologic Research and Minerals of France [*Batu*, 1998, p. 535]. This unconfined aquifer consisted of medium-grained sand with gravel in the deeper part and a clayey matrix at shallow depths. The initial saturated

thickness of the aquifer was 8.24 m. The discharge rate averaged about 53 m³/h and the drawdowns were monitored at a distance of 10 m from the pumping well. The observed drawdown data interpolated by cubic spline had the time interval of one second for each step, for a total of 176,360 data points. Figure 2 demonstrates the data set generated by cubic spline, along with the original 42 data points. The data points form a seemingly S-shaped curve, though its lack of smoothness may be due to the field heterogeneity or measurement errors.

4. Data Analyses and Discussion

4.1. Assessment of Estimation Errors

[31] Two error criteria, mean error and standard error of estimate, are used to assess the errors between the observed and predicted drawdowns.

Table 3. Comparison of Results From Using NLN and EKF

Initial Guess		Convergence	
<i>T</i> m ² /day	<i>S</i>	NLN	EKF
700	0.001	no	yes
700	0.0001	yes	yes
700	0.00001	yes	no
1300	0.001	no	yes
1300	0.0001	yes	yes
1300	0.00001	yes	no
2000	0.001	no	no
2000	0.0001	no	yes
2000	0.00001	yes	no

Table 4. Confined Aquifer Parameters Estimated by Graphical Methods and Their Prediction Errors^a

Methods	Estimated Values		Errors	
	T m ² /day	$S \times 10^{-4}$	ME $\times 10^{-3}$	SEE $\times 10^{-3}$
Theis	1110	2.06	-1.72	8.85
Cooper-Jacob	1090	1.84	-30.96	35.22
Chow	1160	1.93	20.52	22.82

^aSee Yeh [1987].

[32] The mean error (ME) is defined as

$$ME = \frac{1}{n} \cdot \sum_{i=1}^n e_i \quad (28)$$

[33] The principle of least squares assumes that the errors are normally distributed with zero mean and constant variance [McCuen, 1985]. When the ME value is equal to or very close to zero, the assumption that errors have zero mean will be satisfied.

[34] The standard error of estimate (SEE) is defined as

$$SEE = \sqrt{\frac{1}{\nu} \sum_{i=1}^n e_i^2} \quad (29)$$

where ν is the degree of freedom, which equals the number of observed data points minus the number of unknowns.

4.2. Parameter Identification for a Confined Aquifer

[35] For the initial error covariance matrix $P_{k-1}(+)$, the diagonal elements could be first assigned as, for instance, 25000 and 10^{-8} , for T and S , respectively; and the off-diagonal elements of $P_{k-1}(+)$ are set to zero. However, since $P_{k-1}(+)$ equals the expected value of squared estimation error $E[(\hat{x}_{k-1}(+) - x_{k-1})(\hat{x}_{k-1}(+) - x_{k-1})^T]$, a reasonable range for the initial guess for $P_{k-1}(+)$ can be easily obtained. Different cases are assigned different values for $P_{k-1}(+)$. With the computation of the EKF, the values of $P_{k-1}(+)$ are minimized. This means that the estimation errors are gradually reduced step by step, accompanied by the converging state vector $\hat{x}_{k-1}(+)$, i.e., hydraulic param-

eters. The measurement covariance R_k may be set to 10^{-4} or less, remaining constant throughout the filtering process. Given the initial guess values for T and S , along with initial error covariance matrix, the EKF coupled with Theis solution can proceed stepwise to identify the hydraulic parameters. The algorithm is terminated when the specified convergence criteria, according to (12), are all satisfied. The tolerance criterion for T and S are respectively chosen as $TOL_T = 10^{-2}$ (m²/day) and $TOL_S = 10^{-6}$. When those prescribed tolerances are met, the recursive process is terminated and the parameters are then determined.

[36] The two parameters, transmissivity and storage coefficient, are successfully determined in some cases and achieve relatively high accuracy, compared with those estimated by graphical methods, such as the Theis and Cooper-Jacob methods. Nine sets of initial guesses, taken from Yeh [1987], are given for the parameter identification process in order to show the comparison between EKF and NLN. The results by EKF using the nine sets of T and S as initial guesses along with their error estimation are given in Table 1. Note that each time step here is equal to 15 s.

[37] The parameters for some cases are quickly determined and the time steps used for the identification process do not exceed 600 steps, i.e., 2.5 hours of pumping time. An aquifer test with long pumping time is usually conducted to obtain the parameters for confined aquifers by conventional methods. The total pumping time for the recorded data given by Todd [1980] is four hours. Since the EKF only takes about 2.5 hours to obtain the two parameters satisfying the prescribed accuracy, thus the long period of the pumping time may not be required.

[38] In cases 3, 6, and 9, the parameters fail to be determined as indicated in Table 1. In these three cases, the storage coefficient is set as 10^{-5} , which may be too small to be a guess value. The usual value of S ranges from 10^{-3} to 10^{-5} [Walton, 1970]. Thus a guess value of storage coefficient, say $S = 10^{-4}$, is set along with various guess values of transmissivity T are also given. With $S = 10^{-4}$, the range of initial guess for T is much wider, from 100 m²/day to 3000 m²/day, and the EKF always gives good results. Therefore sensible guesses, especially the guess value of storage coefficient, should be made based on the knowledge of the local hydrogeology to facilitate the implementation of the EKF and obtain accurate parameters. This leads to one

Table 5. Unconfined Aquifer Parameters Estimated by EKF With Various Initial Guesses

Case	Initial Guess				NS, ^a s/hr	Estimated Parameters			
	K_r m/s	K_z m/s	S	S_y		$K_r \times 10^{-3}$ m/s	$K_z \times 10^{-5}$ m/s	S	$S_y \times 10^{-2}$
1	6.E-3 ^b	1.E-5	5.E-4	0.1	8689/2.41	2.24	1.63	9.67E-4	3.72
2	9.E-4	1.E-5	5.E-4	0.1	1275/0.35	2.19	1.74	1.01E-3	3.97
3	1.E-3	1.E-4	5.E-4	0.1	1329/0.37	2.25	1.56	9.69E-4	4.10
4	1.E-3	9.E-6	5.E-4	0.1	10966/3.05	2.21	1.68	1.02E-3	3.98
5	1.E-3	1.E-5	4.5E-4	0.1	24568/6.82	2.23	1.64	9.37E-4	3.81
6	1.E-3	1.E-5	5.5E-4	0.1	2121/0.59	2.18	1.76	1.02E-3	4.11
7	1.E-3	1.E-5	5.E-4	0.01	899/0.25	2.18	1.73	9.90E-4	4.38
8	1.E-3	1.E-5	5.E-4	0.05	2422/0.67	2.22	1.69	1.00E-3	3.87
9	1.E-3	1.E-5	5.E-4	0.1	8920/2.48	2.25	1.62	9.66E-4	3.69
10	1.E-3	1.E-5	5.E-4	0.3	8977/2.49	2.24	1.62	9.64E-4	3.70

^aNS represents the number of time steps.

^bRead 6.E-3 as 6×10^{-3} .

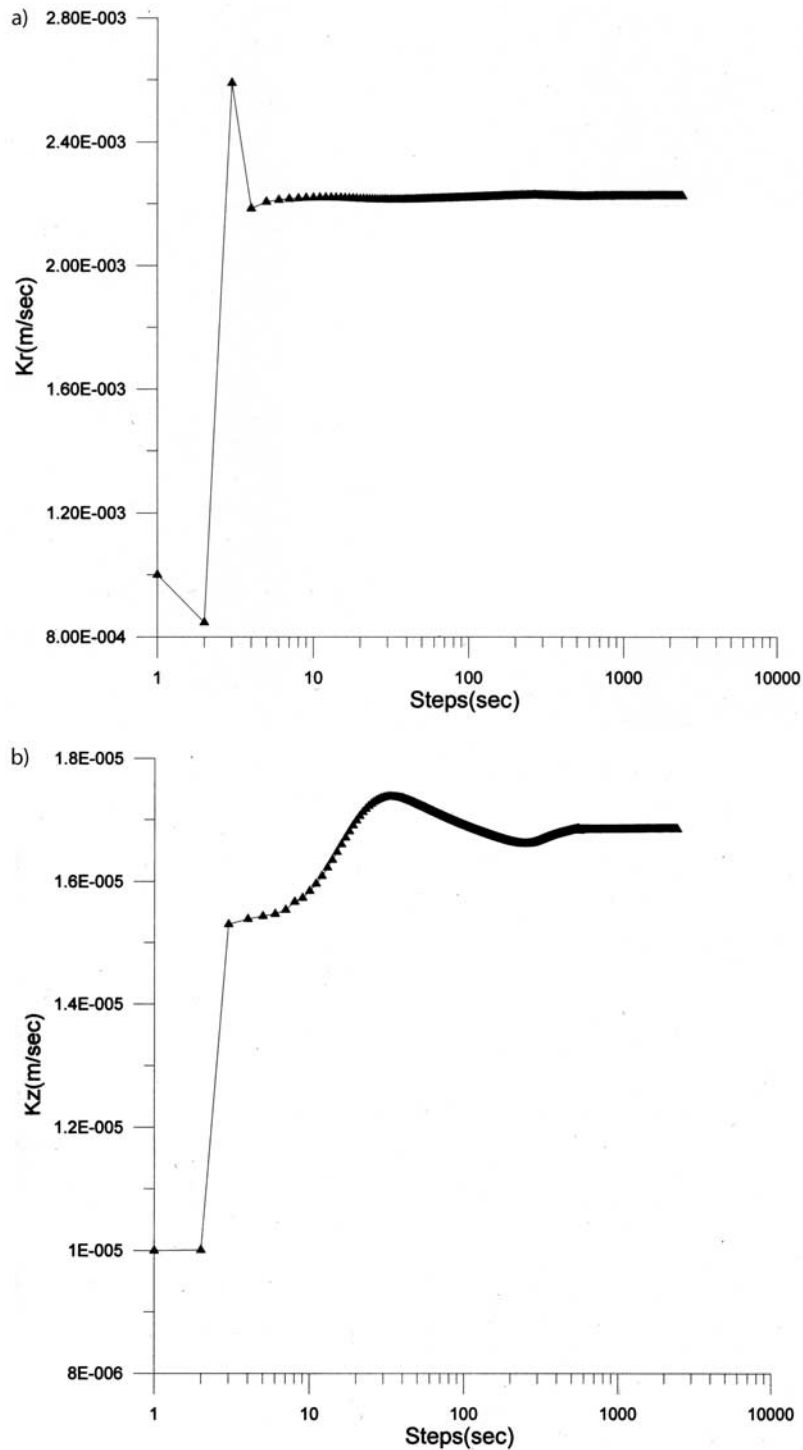


Figure 5. The unconfined aquifer parameter identification process for (a) K_r , (b) K_z , (c) S , and (d) S_y .

inference that assigning a reasonable initial guess S is crucial in applying the EKF. With an initial guess T ranging from $100 \text{ m}^2/\text{day}$ to $3000 \text{ m}^2/\text{day}$ and fixed guess value $S = 10^{-4}$, the estimated parameters and their prediction errors are listed in Table 2. With a reasonable initial guess of S , the EKF allows a wider range of initial guess of T as compared with NLN. The determined T ranges from 1134 to $1157 \text{ m}^2/\text{day}$ averaging $1142 \text{ m}^2/\text{day}$ and the determined S ranges from 1.79×10^{-4} to 1.95×10^{-4} , averaging 1.90×10^{-4} .

Among those six cases, the one with initial guess $T = 500 \text{ m}^2/\text{day}$ has the least SEE value.

[39] Figure 3 shows the estimated T and S for case 8 at each time step. The parameter values change significantly in the early time steps and tend to approach a certain value as the time steps increase. Figure 1 shows a jump in the pumping test data between steps 200 and 320, i.e., between 50 and 80 min after start of pumping. The observed datum measured at 60 min causes the interpolation data between

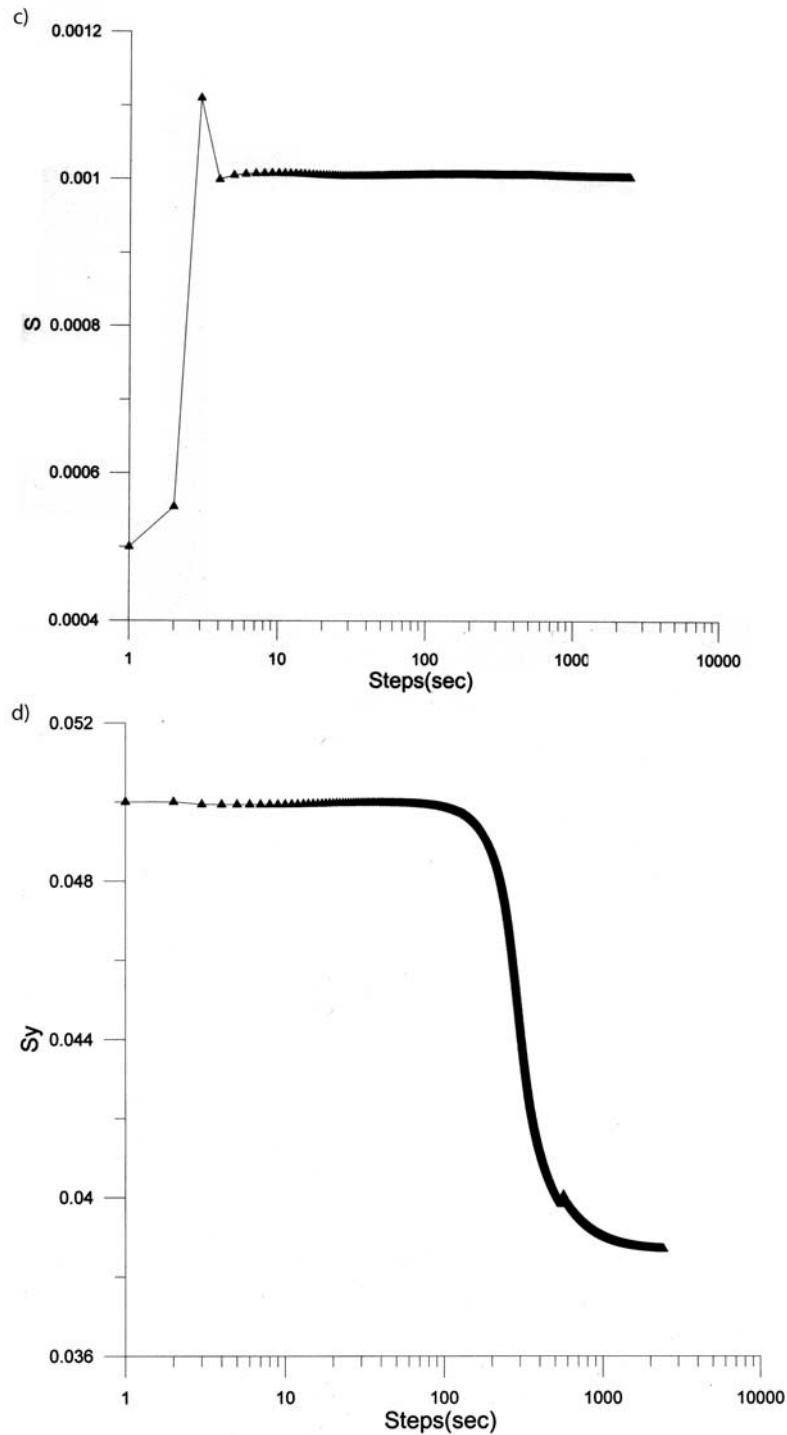


Figure 5. (continued)

step 200 and 320 to form a bump, leading to a fluctuation both in T and S identification process, as displayed in Figure 3. The bump datum does not conform to the Theis behavior, suggesting that the errors embedded in the observation data might temporarily disturb the parameter identification process. Figure 4 shows the observed drawdowns and the computed drawdowns using the estimated parameters obtained from case 8. Figure 4 indicates that the computed drawdowns match the pumping test data quite well.

[40] Table 3 lists the initial guesses for T and S and the estimated results, indicating that both NLN and EKF do not converge in four out of nine cases. The values of parameters obtained by NLN for the four cases are all the same, i.e., $T = 1139 \text{ m}^2/\text{day}$ and $S = 1.93 \times 10^{-4}$. The errors estimated are $ME = 4 \times 10^{-4}$ and $SEE = 5.47 \times 10^{-3}$. Parameter identification employing NLN yields a slightly smaller value of SEE though in the same order of magnitude as that of the EKF, if convergence is achieved. Slightly higher prediction errors for the EKF may be due to the use of

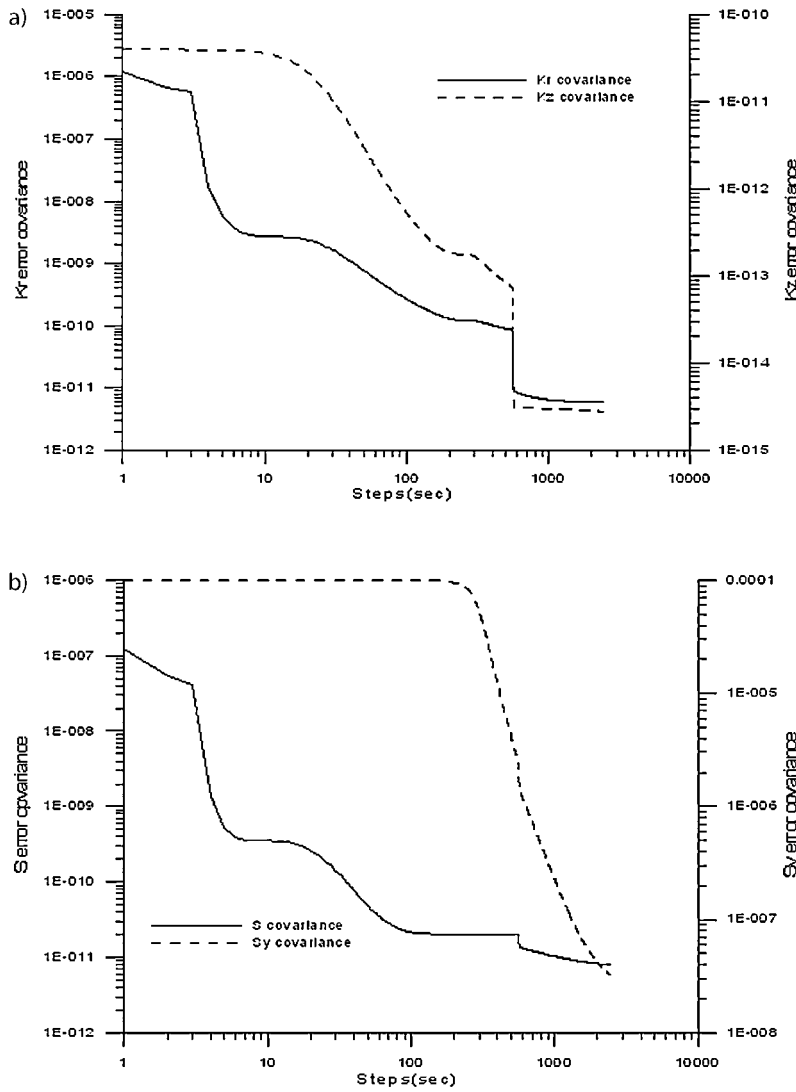


Figure 6. Estimation error covariance of the parameters (a) K_r and K_z and (b) S and S_y .

interpolation data produced by cubic spline, which inevitably introduce additional errors and give slightly less accurate results.

[41] Using conventional graphical methods such as the Theis, Cooper-Jacob, and Chow methods, the analyzed results along with their prediction errors are listed in Table 4 [Yeh, 1987]. The prediction errors of graphical methods are generally larger than those of EKF, as suggested in Tables 2 and 4. Clearly, EKF has the advantage that it avoids erroneous estimation caused by human subjectivity during the curve fitting procedure.

4.3. Parameter Identification for an Unconfined Aquifer

[42] With the off-diagonal elements set to zero, the diagonal elements of initial error covariance matrix $P_{k-1}^{(+)}$ could be assigned the values, for example, say 10^{-6} , 10^{-10} , 10^{-8} and 10^{-3} , for K_r , K_z , S , and S_y , respectively. The measurement covariance R_k might be set to 10^{-6} , remaining constant throughout the identification process. Given the initial values for error covariance matrix and initial guesses for hydraulic parameters, the EKF combined

with the Neuman's model can also identify the hydraulic parameters stepwise. The process of parameter identification usually starts with parameters varying drastically and then the parameters tend to approach constant values asymptotically. The tolerance criteria for K_r , K_z , S , and S_y are respectively chosen as $TOL_{K_r} = 10^{-6}$ (m/s), $TOL_{K_z} = 10^{-8}$ (m/s), $TOL_S = 10^{-6}$ and $TOL_{S_y} = 10^{-5}$ when analyzing the pumping test data in an unconfined aquifer.

[43] Ten sets of the initial guesses are chosen when using the EKF to analyze the drawdown data obtained from a pumping test in the unconfined aquifer discussed above. The estimated results for the ten sets of initial guesses are shown in Table 5. The values determined for K_r range from 2.18×10^{-3} to 2.25×10^{-3} m/s averaging 2.22×10^{-3} m/s. The values determined for K_z range from 1.56×10^{-5} to 1.76×10^{-5} m/s averaging 1.66×10^{-5} m/s. The values determined for S range from 9.37×10^{-4} to 1.02×10^{-3} averaging 9.83×10^{-4} . The values determined for S_y range from 3.69×10^{-2} to 4.38×10^{-2} , with an average of 3.95×10^{-2} . Of the ten cases, case 3 has the least SEE value.

[44] Figure 5 exhibits the values of the parameters for case 8 at each time step to demonstrate the identification process.

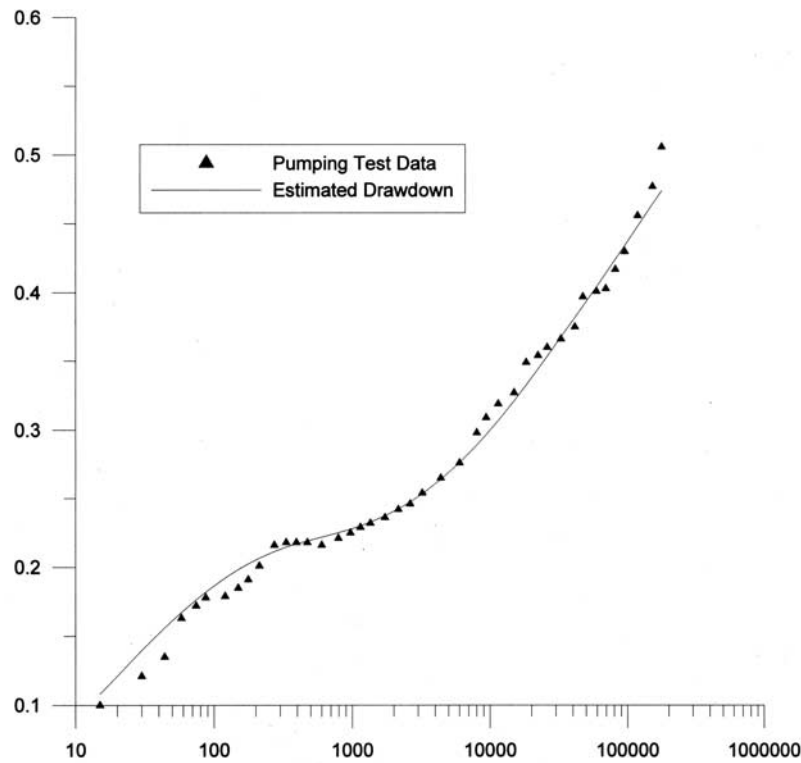


Figure 7. The pumping test data from *Batu* [1998] and the drawdown curve predicted by the estimated parameters.

The parameters, except S_y , vary drastically at the beginning and then asymptotically approach constant values during the identification process. Figure 6 shows the covariances of the state estimation errors for case 8. The error covariance plots for K_r and S demonstrate rapid decrease during the first five steps and then mild decrease thereafter. Both plots exhibit roughly similar shape and indicate that the estimated parameters tend to converge after about 560 steps. The error covariance of K_z and S_y seems to initially remain constant and then decreases rapidly after some steps. Figure 7 displays the plots of the observed and predicted drawdowns using the estimated parameters of case 8, indicating that the predicted drawdowns closely match the pumping test data. The EKF approach successfully determines the four hydraulic parameters in all cases and has the advantage of good accuracy, judging from the values of ME and SEE listed in Table 6.

[45] The parameter values for all cases are determined when the tolerance criteria are met. The total time steps used in the recursive process for those ten cases do not exceed 25000 steps, i.e. 25000 s (6.94 hours). In engineering practice, it is commonly recognized that a pumping test for an unconfined aquifer should be conducted for more than one day so that the recorded data can include the effect of gravity yield. The chosen pumping test for analyses in this paper lasted about 49 hours [*Batu*, 1998, p. 535]. The analyzed results imply that a 7 hour period may be sufficient for the unconfined pumping test when using the EKF for data analyses. Therefore excess time spent in pumping test may be saved if the EKF approach is employed.

[46] Table 7 lists the values of initial guesses and the analyzed results of using the NLN and EKF. Four out of ten cases for NLN do not converge, while all cases for the

EKF converges. The results obtained by NLN for the four cases are: $K_r = 2.22 \times 10^{-3}$ m/s, $K_z = 1.68 \times 10^{-5}$ m/s, $S = 1.31 \times 10^{-3}$, and $S_y = 3.85 \times 10^{-2}$ and the prediction errors are $ME = 2.76 \times 10^{-4}$ and $SEE = 8.06 \times 10^{-3}$. Although NLN converges more quickly than EKF and the estimated parameters have slightly less estimation errors, the EKF, on the other hand, has wider range of initial guesses and the prediction error of SEE is in the same order of magnitude as that of NLN. Table 8 lists the analyzed results and the prediction errors from the graphical approaches such as the Neuman type-curve method and Neuman’s semilogarithmic method [*Batu*, 1998]. The prediction errors from using the EKF are generally much smaller than those by these two graphical methods, indicating a better fit for the drawdown data.

[47] When the drawdown data are plotted against time in logarithmic scale, the curve of these data has an S-shape

Table 6. Prediction Errors for the Determined Parameters in an Unconfined Aquifer

Case	ME $\times 10^{-3}$	SEE $\times 10^{-3}$
1	-2.65	9.73
2	-3.87	9.77
3	1.68	8.36
4	-2.42	9.43
5	3.10	10.16
6	-3.47	9.67
7	-2.19	10.06
8	-1.96	9.38
9	-2.05	9.67
10	-2.97	9.81

Table 7. Comparison of NLN and EKF With the Same Initial Guess Values

Case	Initial Guess				Convergence	
	K_r , m/s	K_z , m/s	S	S_y	NLN	EKF
1	6.E-3	1.E-5	5.E-4	0.1	no	yes
2	9.E-4	1.E-5	5.E-4	0.1	yes	yes
3	1.E-3	1.E-4	5.E-4	0.1	no	yes
4	1.E-3	9.E-6	5.E-4	0.1	no	yes
5	1.E-3	1.E-5	4.5E-4	0.1	yes	yes
6	1.E-3	1.E-5	5.5E-4	0.1	yes	yes
7	1.E-3	1.E-5	5.E-4	0.01	no	yes
8	1.E-3	1.E-5	5.E-4	0.05	yes	yes
9	1.E-3	1.E-5	5.E-4	0.1	no	yes
10	1.E-3	1.E-5	5.E-4	0.3	no	yes

consisting of a steep segment at early times, a relatively flat segment at middle times (indicating small drawdowns), and a steeper segment again at late times, as shown in Figure 7. At early times, the water comes from the elastic behavior of the water and aquifer formation and this early steep portion of the curve is attributed to the storage coefficient equivalent of a confined aquifer. The physical phenomenon that causes the flat segment at moderate times is the gravity drainage replenishment. At late times, the steep portion of the curve can be described by specific yield S_y , also following the Theis curve with $S = S_y$. The change of S_y value during the identification process exhibits a phenomenon that can be related to the aquifer physical behavior. Figure 8 illustrates the values of S_y during the identification process for cases 7–10 listed in Table 4. Specific yields, S_y , are often in the range of 0.01 to 0.3 [Batu, 1998]. Thus the values of S_y chosen as initial guesses for the four cases are 0.01, 0.05, 0.1, and 0.3, and the rest of the guess parameters are $K_r = 1.0 \times 10^{-3}$ m/s, $K_z = 1.0 \times 10^{-5}$ m/s, and $S = 5.0 \times 10^{-4}$ for all cases. The value of specific yield S_y during the recursive process does not change much initially (say, within 100 s) as indicated in Figure 8, because the elastic behavior of the aquifer dominates and nothing to do with the gravity drainage. In the flat segment of the pumping data, the guess value for S_y starts to vary after 100 steps, (i.e., 100 s) implying that the gravity drainage plays an important role during this period of time. All of the cases show the same phenomenon, which concludes the flat segment is the crucial transition stage for this particular parameter. At late times the S_y value for all cases converges to a certain value, demonstrating that the identification process of the EKF for S_y can reflect the physical nature of the unconfined aquifer.

4.4. Analyses for Drawdown Data With Uncorrelated and Temporally Correlated Noises

[48] The MATLAB function `randn(m, n)` with $m = 500$ and $n = 1$ is first chosen to generate a realization of white

noises [The MathWorks, 1995]. The elements in this realization are normally distributed random numbers with zero mean and unit variance. Each element is then multiplier by 8.29×10^{-3} , which is calculated based on the data variance (0.942) and the SEE value of case 3 (8.36×10^{-3}). Finally, 420 data point is taken from this realization and divided into ten data sets. Therefore each data set contains 42 elements (i.e., 42 data points). Neuman’s model along with the parameters estimated from case 3 by the EKF was employed to generate 42 predicted drawdown data points. Thus a set of pumping drawdown data was synthesized by simply adding the adjusted noise data to the predicted drawdown data one by one. Accordingly ten sets of synthetic drawdown data with uncorrelated noises were obtained.

[49] The original realization of white noises is employed to generate temporally correlated noises. The MATLAB function `hamming(n)` with $n = 5$ is used to produce five coefficients of a Hamming window [The MathWorks, 1995]. The MATLAB function `conv(a, b)` is applied to convolves vectors a and b [The MathWorks, 1995], where vector a represents the original realization and vector b represents the coefficients of the Hamming window. Algebraically, convolution can be thought of as multiplying the polynomials whose coefficients are the elements of a and b . Each element of the product of the convolution is adjusted by a factor of 6.57×10^{-3} , which is calculated based on the data variance (1.500) and the SEE value of case 3. The result after the adjustment represents a new realization with temporally correlated noises. Thus ten sets of synthetic drawdown data with temporally correlated noises can be formed in a similar manner to the procedure of generating the drawdown data with uncorrelated noises. The initial guesses for the hydraulic parameters are: $K_r = 1 \times 10^{-3}$ m/s, $K_z = 1 \times 10^{-5}$ m/s, $S = 1 \times 10^{-3}$, and $S_y = 1 \times 10^{-2}$. The analyzed results by EKF are listed in Table 9, indicating that the EKF may also be applicable for data with white noises and temporally correlated noises, although the prediction errors of SEE are slightly higher than those when analyzing the real drawdown data.

5. Conclusions

[50] An approach using the EKF and cubic spline is proposed to identify the hydraulic parameters in both confined and unconfined aquifer systems. The EKF combined with the Theis solution can optimally determine the parameters for confined aquifers in the identification process. The drawdown data with nonuniform time intervals from the pumping test are interpolated by cubic spline to have uniform time interval. This interpolation approach facilitates the implementation of EKF. In an unconfined system, Neuman’s model is employed in the same manner as the Theis solution to determine the hydraulic parameters.

Table 8. Unconfined Aquifer Parameters Estimated by Graphical Methods and Their Prediction Errors

Methods	Estimated Values				Errors	
	$K_r \times 10^{-3}$, m/s	$K_z \times 10^{-3}$, m/s	$S \times 10^{-3}$	$S_y \times 10^{-2}$	ME $\times 10^{-3}$	SEE $\times 10^{-3}$
Neuman type curve	2.4	1.62	1.46	5.73	32.90	34.59
Neuman semilogarithmic	2.4	1.62	1.87	2.13	14.23	14.96

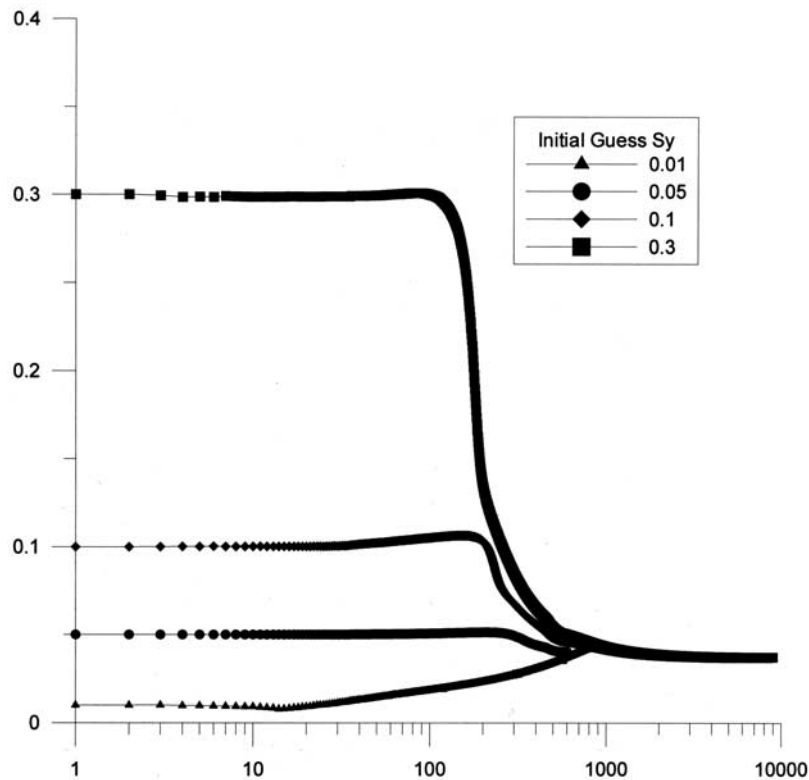


Figure 8. Change of S_y in the identification process for different initial guesses.

[51] Using only a few observed drawdown data, the proposed approach can quickly identify the parameters. In the confined aquifer, the estimated parameters can be obtained within 150 min (2.5 hours) for some cases and have small prediction errors. For most cases in unconfined systems, the EKF can determine the hydraulic parameters and achieve good accuracy within seven hours. In contrast, pumping tests lasting more than one day are commonly considered necessary to include the effect of gravity yield. However, the analyzed results by the EKF imply that a few hours may be enough for an unconfined pumping test. At present, pumping tests are usually performed in the field with a system having pressure transducers installed in the observation wells to measure the water level and a data logger to store the measured data transmitted from the pressure transducers. Such a system may be linked to a computer in which the EKF coupled with the aquifer model is implemented and executed simultaneously. Accordingly, the hydraulic parameters can be determined on-line in the field. Once stable estimates of the hydraulic parameters have been reached, the pumping test may be terminated.

[52] Results of using NLN and EKF for analyzing the pumping test data with various initial guess values are analyzed and compared. In confined cases, the EKF allows a wide range for the initial guess T , when an initial guess value of S is given closer to the actual S . The EKF is shown to have a wider range of initial guess values than NLN in unconfined cases, though the accuracy by employing NLN is slightly higher. In terms of graphical methods, in both confined and unconfined cases, graphical methods have larger prediction errors than the EKF. Clearly, the EKF can avoid the inaccuracy caused by human subjectivity during the curve fitting procedure.

[53] The MATLAB function $\text{randn}(m, n)$ and the Neuman’s model along with the parameters estimated from case 3 by the EKF are employed to generate ten sets of synthetic drawdown data with uncorrelated noises. Also the MAT-

Table 9. Results From Analyzing the Drawdown Data With White Noise and With Temporally Correlated Noise

Case	$Kr \times 10^{-3}$, m/s	$Kz \times 10^{-5}$, m/s	$S \times 10^{-4}$	$S_y \times 10^{-2}$	SEE $\times 10^{-2}$	NS ^a
<i>Drawdown Data With White Noise</i>						
1	NA ^b	NA	NA	NA	NA	NA
2	2.29	2.00	9.89	0.52	7.89	291
3	2.32	1.81	9.48	2.20	1.61	1282
4	2.82	0.81	7.46	1.37	1.40	6376
5	2.17	2.29	9.85	1.44	5.10	432
6	2.44	1.80	9.65	0.61	5.32	407
7	2.28	1.14	10.00	1.06	5.34	20
8	NA	NA	NA	NA	NA	NA
9	3.16	0.74	9.98	0.04	5.34	805
10	NA	NA	NA	NA	NA	NA
<i>Drawdown Data With Temporally Correlated Noise</i>						
1	2.66	1.04	7.74	1.37	0.79	11854
2	2.44	1.83	9.77	0.62	5.35	293
3	2.54	1.27	8.83	2.15	0.69	2786
4	NA	NA	NA	NA	NA	NA
5	NA	NA	NA	NA	NA	NA
6	NA	NA	NA	NA	NA	NA
7	2.27	2.13	9.77	1.24	4.54	231
8	2.14	2.12	9.69	2.80	2.57	1629
9	2.46	1.62	9.71	1.14	2.82	937
10	NA	NA	NA	NA	NA	NA

^aNS represents the number of the time steps.

^bNA represents that the result is not available under the specified tolerance criteria.

LAB functions $\text{hamming}(n)$ and $\text{conv}(a, b)$ with the same Neuman's model are used to generate ten sets of synthetic drawdown data with temporally correlated noises. The analyzed results indicate that EKF can successfully analyze data with white noises or temporally correlated noises, although the prediction errors are slightly higher than those when analyzing the real drawdown data.

Appendix A: Evaluation of H_k

A.1. Theis Equation

[54] Based on (15) and (16), and Leibnitz rule [Wylie and Barrett, 1995], the two derivatives $\partial\hat{x}_k/\partial T$ and $\partial\hat{x}_k/\partial S$ in (20) can be directly derived as

$$\frac{\partial\hat{z}_k}{\partial T} = \frac{q}{4\pi T^2}(e^{-u} - W(u)) \quad (\text{A1})$$

and

$$\frac{\partial\hat{z}_k}{\partial S} = -\frac{q}{4\pi TS}e^{-u} \quad (\text{A2})$$

A.2. Neuman's Model

[55] In Neuman's four-parameter model, the values of drawdown depend on the decisive variables, K_r , K_z , S , and S_y , which may be written as

$$s = \frac{q}{4\pi T} \cdot G(K_r, K_z, S, S_y) \quad (\text{A3})$$

where $G(K_r, K_z, S, S_y)$ represents the integral in (22).

[56] The four derivatives $\partial\hat{x}_k/\partial K_r$, $\partial\hat{x}_k/\partial K_z$, $\partial\hat{x}_k/\partial S$, and $\partial\hat{x}_k/\partial S_y$ are

$$\frac{\partial\hat{z}_k}{\partial K_r} = -\frac{q}{4\pi K_r^2 b}G + \frac{q}{4\pi T} \frac{\partial G}{\partial K_r} \quad (\text{A4})$$

$$\frac{\partial\hat{z}_k}{\partial K_z} = \frac{q}{4\pi K_r b} \frac{\partial G}{\partial K_z} \quad (\text{A5})$$

$$\frac{\partial\hat{z}_k}{\partial S} = \frac{q}{4\pi K_r b} \frac{\partial G}{\partial S} \quad (\text{A6})$$

$$\frac{\partial\hat{z}_k}{\partial S_y} = \frac{q}{4\pi K_r b} \frac{\partial G}{\partial S_y} \quad (\text{A7})$$

where $\partial G/\partial K_r$ is approximated by forward differencing as

$$\frac{\partial G}{\partial K_r} = \frac{G(K_r + \Delta K_r, K_z, S, S_y) - G(K_r, K_z, S, S_y)}{\Delta K_r} \quad (\text{A8})$$

and the other partial derivatives $\partial G/\partial K_z$, $\partial G/\partial S$, and $\partial G/\partial S_y$ are also expressed in a similar manner. The increment shown in the denominator may be approximated by the parameter value times a factor of 10^{-3} or less, e.g., $\Delta K_r = 10^{-3}K_r$.

[57] **Acknowledgments.** This study was partly supported by the Taiwan National Science Council under grant NSC89-2621-Z-009-006.

The authors would also like to thank the two anonymous reviewers for their valuable and constructive comments. We are also grateful to Yen-Chen Huang for his help in preparing Table 9 and Figure 6.

References

- Batu, V., *Aquifer Hydraulics*, John Wiley, New York, 1998.
- Bierkens, M. F. P., Modeling water table fluctuations by means of a stochastic differential equation, *Water Resour. Res.*, 34, 2485–2499, 1998.
- Bierkens, M. F. P., M. Knotters, and T. Hoogland, Space-time modeling of water depth using a regionalized time series model and the Kalman filter, *Water Resour. Res.*, 37, 1277–1290, 2001.
- Boulton, N. S., Unsteady radial flow to a pumped well allowing for delayed yield from storage, *IASH Publ.*, 37, 472–477, 1954.
- Boulton, N. S., Analysis of data from non-equilibrium pumping tests allowing for delayed yield from storage, *Proc. Inst. Civ. Eng.*, 26, 469–482, 1963.
- Burden, R. L., and J. D. Faires, *Numerical Analysis*, Brooks/Cole, Pacific Grove, Calif., 1997.
- Cahill, A. T., F. Ungaro, M. B. Parlange, M. Mata, and D. R. Nielsen, Combined spatial and Kalman filter estimation of optimal soil hydraulic properties, *Water Resour. Res.*, 35, 1079–1088, 1999.
- Chander, S., P. N. Kapoor, and S. K. Goyal, Aquifer parameter estimation using Kalman filters, *J. Irrig. Drain. Div. Am. Soc. Civ. Eng.*, 107, 25–33, 1981.
- Chow, V. T., On the determination of transmissibility and storage coefficients from pumping test data, *Eos Trans. AGU*, 33, 397–404, 1952.
- Cooley, R. L., and C. M. Case, Effect of a water-table aquitard on drawdown in an underlying pumped aquifer, *Water Resour. Res.*, 9, 434–447, 1973.
- Cooper, H. H. Jr., and C. E. Jacob, A generalized graphical method for evaluating formation constants and summarizing well field history, *Eos Trans. AGU*, 27(IV), 526–534, 1946.
- Eigbe, U., M. B. Beck, H. S. Wheatler, and F. Hirano, Kalman filtering in groundwater flow modelling: Problems and prospects, *Stochastic Hydrol. Hydraul.*, 12, 15–32, 1998.
- Gerald, C. F., and P. O. Wheatley, *Applied Numerical Analysis*, 5th ed., Addison-Wesley-Longman, Reading, Mass., 1994.
- Grewal, M. S., and A. P. Andrews, *Kalman Filtering: Theory and Practice*, Prentice-Hall, Old Tappan, N. J., 1993.
- Huang, W. C., A numerical method for determining parameters of unconfined aquifer, MS. thesis, Inst. of Environ. Eng., Natl. Chiao-tung Univ., Hsinchu, Taiwan, 1996.
- Katul, G. G., O. Wendroth, M. B. Parlange, C. E. Puente, M. V. Folegatti, and D. R. Nielsen, Estimation of in situ hydraulic conductivity function from nonlinear filtering theory, *Water Resour. Res.*, 29, 1063–1070, 1993.
- Lee, Y. P., C. V. Chin, and P. H. Yen, Application of Kalman filter for real-time identifying aquifer anisotropy, in paper presented at the 11th Hydraulic Engineering Conference, Natl. Taiwan Univ., Taipei, Taiwan, 2000.
- McCuen, R. H., *Statistical Methods for Engineers*, Prentice-Hall, Old Tappan, N. J., 1985.
- Moench, A. F., Combining the Neuman and Boulton models for flow to a well in an unconfined aquifer, *Ground Water*, 33, 378–384, 1995.
- Neuman, S. P., Theory of flow in unconfined aquifers considering delayed response of the water table, *Water Resour. Res.*, 8, 1031–1044, 1972.
- Neuman, S. P., Effects of partial penetration on flow in unconfined aquifers considering delayed aquifer response, *Water Resour. Res.*, 10, 303–312, 1974.
- Neuman, S. P., Analysis of pumping test data from anisotropic unconfined aquifers considering delayed gravity response, *Water Resour. Res.*, 11, 329–342, 1975.
- Prickett, T. A., Type-curve solution to aquifer tests under water-table conditions, *Ground Water*, 3, 5–14, 1965.
- The MathWorks, *The Student Edition of MATLAB, Version 4, User's Guide*, Prentice-Hall, Old Tappan, N. J., 1995.
- Theis, C. V., The relation between the lowering of the piezometric surface and the rate and duration of discharge of a well using ground-water storage, *Eos Trans. AGU*, 16, 519–524, 1935.
- Todd, D. K., *Ground Water Hydrology*, 2nd ed., 535 pp., John Wiley, New York, 1980.
- Van Geer, F. C., and C. B. M. te Stroet, A Kalman filter approach to the quantification of the reliability of a groundwater model, in *Calibration and Reliability in Groundwater Modeling*, edited by K. Kovar, *IASH Publ.*, 195, 467–476, 1990.

- Van Geer, F. C., and P. Van Der Kloet, Two algorithms for parameter estimation in groundwater flow problems, *J. Hydrol.*, 77, 361–378, 1985.
- Van Geer, F. C., C. B. M. te Stroet, and M. F. P. Bierkens, Groundwater modeling in relation to the system's response time using Kalman filtering, in *Computational Methods in Subsurface Hydrology: Proceedings of the Eighth International Conference*, edited by G. Gambolati, et al., part A, pp. 23–30, Springer-Verlag, New York, 1990.
- Walton, W. C., *Groundwater Resource Evaluation*, McGraw-Hill, New York, 1970.
- Wylie, C. R., and L. C. Barrett, *Advanced Engineering Mathematics*, McGraw-Hill, New York, 1995.
- Yeh, H. D., Theis' solution by nonlinear least-squares and finite-difference Newton's method, *Ground Water*, 25, 710–715, 1987.
-
- C. H. Leng and H. D. Yeh, Institute of Environmental Engineering, National Chiao-Tung University, Number 75, Po-Ai Street, Hsinchu, 300, Taiwan. (hdyeh@mail.nctu.edu.tw)